Materials Science and Engineering A 423 (2006) 84–91

MATERIALS SCIENCE & ENGINEERING A

www.elsevier.com/locate/msea

QM/MM and classical molecular dynamics simulation of histidine-tagged peptide immobilization on nickel surface

Zhenyu Yang, Ya-Pu Zhao *

State Key Laboratory of Nonlinear Mechanics (LNM), Institute of Mechanics, Chinese Academy of Sciences, Beijing 100080, People's Republic of China

Received 8 July 2005; received in revised form 22 September 2005; accepted 15 October 2005

Abstract

The hybrid quantum mechanics (QM) and molecular mechanics (MM) method is employed to simulate the His-tagged peptide adsorption to ionized region of nickel surface. Based on the previous experiments, the peptide interaction with one Ni ion is considered. In the QM/MM calculation, the imidazoles on the side chain of the peptide and the metal ion with several neighboring water molecules are treated as QM part calculated by "GAMESS", and the rest atoms are treated as MM part calculated by "TINKER". The integrated molecular orbital/molecular mechanics (IMOMM) method is used to deal with the QM part with the transitional metal. By using the QM/MM method, we optimize the structure of the synthetic peptide chelating with a Ni ion. Different chelate structures are considered. The geometry parameters of the QM subsystem we obtained by QM/MM calculation are consistent with the available experimental results. We also perform a classical molecular dynamics (MD) simulation with the experimental parameters for the synthetic peptide adsorption on a neutral Ni(1 0 0) surface. We find that half of the His-tags are almost parallel with the substrate, which enhance the binding strength. Peeling of the peptide from the Ni substrate is simulated in the aqueous solvent and in vacuum, respectively. The critical peeling forces in the two environments are obtained. The results show that the imidazole rings are attached to the substrate more tightly than other bases in this peptide.

Keywords: Hybrid QM/MM simulation; IMOMM; CHARMM; Histidine; Chelate; Adhesion

1. Introduction

For the nanomechanical systems and the fabrication of biosensors, the immobilization of biomolecules on substrates is a potentially important prerequisite. For instance, self-assembled monolayers (SAMs) are the ordered molecule assemblies that are formed by adsorption to a solid surface. The strong chemisorption of the head-group on the substrate combined with the interactions between the molecules are believed to be at the origin of the spontaneous self-assembly, ultimately leading to a well-ordered film of defined composition. The head-group of a peptide or protein plays a crucial role in the adhesion.

"His-tags" are used in nanomechanical systems and biosensors due to their functional side chains. Noji et al. [1] exploited the high affinity of polyhistidine-tagged β-subunits for Ni–nitrilotriacetate (NTA) to immobilize an F1-ATPase $\alpha_3\beta_3\gamma$ subcomplex on a solid surface (Fig. 1). They found that the polyhistidine tags were bound so tightly to the Ni–NTA HRP Conjugate that $\alpha_3\beta_3\gamma$ subcomplex were immobilized even under the high torque produced by the rotating actin filaments. In order to specifically attach, as well as precisely position and orient, biological molecules on metal substrates, His-tags were used by Montemagno et al. [2] to attach a biomolecular motor, F1-ATPase, to metal substrates, and they have tested the binding strength of a 6 × His-tagged synthetic peptide attached to Au-, Cu- and Ni-coated coverslips.

The nitrogen atom in the imidazole of histidine has one pair of electrons, which can be donated to a metal ion, especially transitional metal ion. This nitrogen atom that is directly bonded to the metal ion/atom is called the donor atom, with a coordinate covalent bond formed between the two atoms. A coordination compound in which a heterocyclic ring is formed by a metal bound to two atoms of the associated ligand can be defined as chelate complexes. A visual sketch map for the chelation by R.J. Lancashire is shown in Fig. 2 in which a lobster holds a metal ion indicating a heterocyclic ring. Hochuli et al. [3] applied histidine

* Corresponding author. Tel.: +86 10 6265 8008; fax: +86 10 6256 1284.
E-mail address: yzhao@lnm.imech.ac.cn (Y.-P. Zhao).

0921-5093/$ – see front matter © 2006 Elsevier B.V. All rights reserved.
doi:10.1016/j.msea.2005.10.078

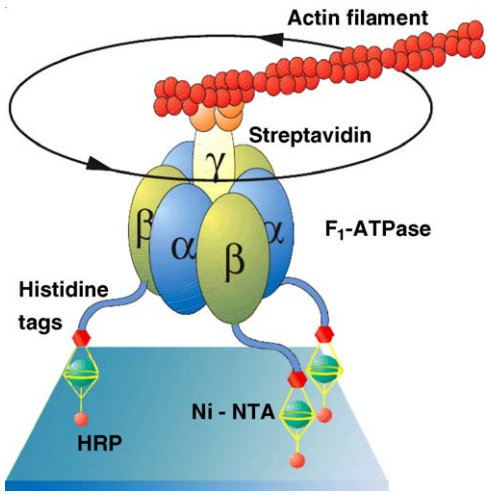

Fig. 1. Immobilization of F1-ATPase $\alpha_3\beta_3\gamma$ subcomplex on solid surface by polyhistidine interaction with Ni–NTA [1].

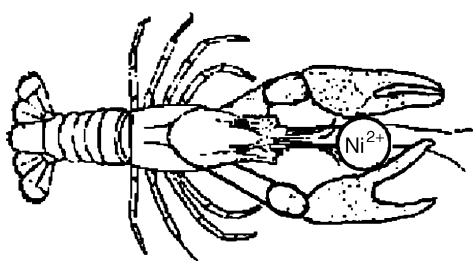

Fig. 2. A visual sketch map of chelation.

in selective binding proteins when they discovered that proteins containing isolated histidines lead to complexes that are less stable than those arising from proteins having two consecutive His-tags at one terminus (2 × His-tag). Indeed, a stretch of six consecutive His tags (6 × His-tag) is now commonly appended to the primary sequence of recombinant proteins, making it possible to immobilize them on biosensors for biomolecular interaction analysis [4]. His-tagged peptide has been chosen due to its relevance in many biological processes and for its particular side chain. The imidazole ring shown in Fig. 3 is involved in enzyme catalysis and in the binding of metal ions to proteins as a result of its ability to gain or lose a proton at physiological pH values.

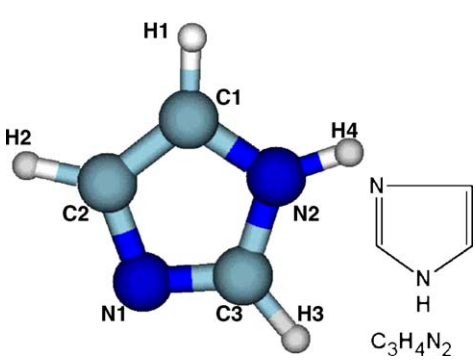

Fig. 3. The structure of imidazole ring and molecular formula.

In order to link biomolecules to solids, Nuzzo and Allara. [5] bound thiols to gold involving covalent interaction. Demers et al. [6] immobilized acrylamides on silanized surfaces. Agarwal et al. [7] demonstrated that polyhistidine-tagged peptides and proteins, and free-base porphyrins coated on AFM probes, can be chelated to ionized regions on a metallic Ni surface by applying an electric potential to the AFM tip in the Dip-pen nanolithography (DPN) process. In the DPN experiments, when the probes coated with the His-tagged peptide and zero potential on a Ni surface, no deposition was observed. After the potential applied between the probe and substrate, Ni surface changes to be ionized, then six His-tagged peptide/protein attaches to the ionized Ni surface. So some immobilizations via naturally occurring electrostatic attraction is unsuitable for some device applications. The molecular forces of the complex bonds of the Ni^{2+}–NTA/His-tag complex at a constant loading rate of 0.5 μm/s have been obtained by Schmitt et al. [8]. The coordination bond between a histidine tag and Ni–NTA has been studied experimentally at mechanochemistry level [9]. All the experiments validate that imidazole nitrogen donor atoms coordinate with Ni ion and form strong bonds.

Besides the function in immobilization, histidine residues have two different roles in metalloenzymes: it can coordinate the metal ion through its imidazole nitrogen or, alternatively, upon deprotonation of the pyrrole nitrogen, it may act as a bridging ligand between two metal centers. Protein tagged with six histidine (His_6) residues can be purified by metal chelate chromatography. Metal chelate chromatography is based on the complexing of metal ions as Ni^{2+}, Cu^{2+} or Co^{2+} immobilized by chelate formation through imidazole ring of the amino acid histidine.

At the beginning of simulation for the bio-chemical systems, quantum mechanics (QM) and molecular mechanics (MM) are usually utilized separately. QM method has the advantage over MM method that it includes the effects of charge transfer, polarization and bond breaking and forming from the beginning. So QM simulation is employed for the investigation of the chemical reaction, while MM simulation method is well suited for the investigation of the transformation of the conformation in large system. But the computation cost of QM method is so expensive. While, combining both merits of QM and MM, MM method has been coupled to QM method leading to hybrid QM/MM algorithm [10], which models a very large system using MM and on crucial section of the system with QM. This is designed to give results that have very good speed where only one region needs to be modeled quantum mechanically.

General Atomic and Molecular Electronic Structure System (GAMESS) [11] is a general ab initio quantum chemistry package. It can compute self-consistent field (SCF) wavefunctions ranging from restricted Hartree Fock (RHF), restricted open shell Hartree Fock (ROHF), unrestricted Hartree Fock (UHF), to generalized valence bond (GVB) and multi-configurational self-consistent field (MCSCF). Correlation corrections to these SCF wavefunctions include density functional theory (DFT) approximation, configuration interaction, etc. For automatic geometry optimization, analytic gradients are available. There is an optional QM/MM add-on module available for GAMESS, based on the classical molecular dynamics (MD) software TINKER

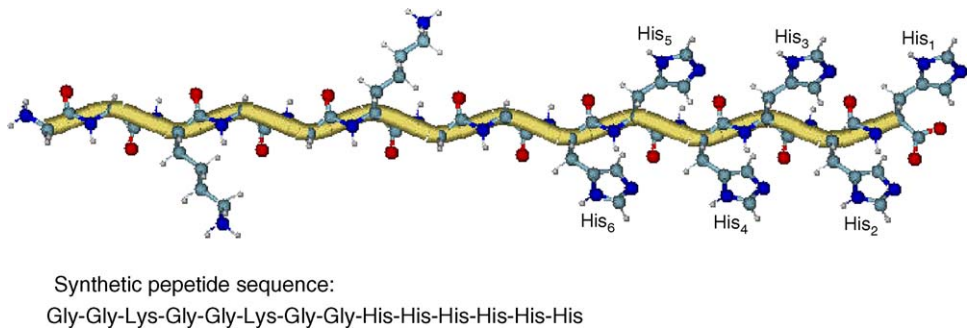

Fig. 4. The synthetic peptide with 6 × His-tags. The blue atoms are nitrogen atoms, the white ones are hydrogen atoms, the red ones are oxygen atoms and the rest are carbon atoms.

program [12]. GAMESS/TINKER can perform the Integrated Molecular Orbital/Molecular Mechanics (IMOMM) scheme [13], which spearheads the entry of hybrid QM/MM approaches in computational transition metal chemistry. The validity of the IMOMM method for accurate calculation of the transition metal complexes has been affirmed [14].

This novel technique of combining a QM treatment of the interested section with a MM treatment of the rest section has given rise to a large number of investigations due to the challenging technological applications in the field of biochemistry and biocatalysis. Many researchers have made progresses in applying the combined QM/MM methods to chemical reaction and catalysis in solution [15–18]. To the authors' knowledge, no work has been done in applying such methods to peptide/protein chemisorption with Ni ion or Ni surface for immobilization.

This work focuses on the 6 × His-tagged synthetic peptide [2] (Fig. 4) attachment to the ionized region in Ni substrate, i.e. the peptide chelating with Ni ion [5], and only one Ni^{2+} ion is considered in this work. GAMESS and TINKER are employed for the QM/MM calculation of the His-tagged peptide chelating with Ni^{2+} ion. The different geometries of the possibly chelating are optimized. The binding energy of the peptide with the Ni ion is obtained at HF(6–31G*)(namely, an extended basis set with polarization basis functions)/MM and B3LYP [19–21] (6–31G*)/MM level, respectively. And we also implement classical MD to simulate this synthetic peptide adsorption to Ni(1 0 0) surface in the aqueous solvent and in vacuum, respectively. The critical peeling force of the peptide peeled off from the Ni substrate is obtained.

2. QM/MM schemes

2.1. Governing equations

The basic strategy for the QM/MM method lies in the hybrid potential in which a classical MM potential is combined with a QM one [10]. The energy of the system, E, is calculated by solving the Schrödinger equation with an effective Hamiltonian, H_{eff}, for the mixed quantum mechanical and classical mechanical system

$$H_{\text{eff}}\psi(r, R_{\text{QM}}, R_{\text{MM}}) = E(R_{\text{QM}}, R_{\text{MM}})\psi(r, R_{\text{QM}}, R_{\text{MM}}) \quad (1)$$

where ψ is the electronic wave function of the quantum system, r is for the coordinates of the electrons, R_{QM} is the position of the quantum mechanical nuclei, as well as R_{MM} is for the molecular mechanical nuclei. The wave function, ψ, depends directly on r, R_{QM} and R_{MM}.

The effective Hamiltonian for the mixed quantum and classical system is divided into three terms [22]

$$H_{\text{eff}} = H_{\text{QM}} + H_{\text{MM}} + H_{\text{QM/MM}} \quad (2)$$

where H_{QM} is the contribution from complete QM section (QM in Fig. 5), H_{MM} is from the pure MM section (MM in Fig. 5) and $H_{\text{QM/MM}}$ is the interaction between the QM and MM portions of the system.Similarly, the total energy of the system calculated by solving the Schrödinger equation can likewise be divided into three component parts

$$E_{\text{eff}} = E_{\text{QM}} + E_{\text{MM}} + E_{\text{QM/MM}}. \quad (3)$$

While, the pure MM term can be removed from the integral because it is independent of the electronic positions. So another way to express the total energy of the system is as the expectation value of H_{eff} [23]

$$E_{\text{eff}} = \langle\psi|H_{\text{QM}} + H_{\text{QM/MM}}|\psi\rangle + E_{\text{MM}} \quad (4)$$

in which, H_{QM} is the Hamiltonian that can be obtained by either semiempirical, Hartree Fock, or DFT, while E_{MM} is an energy got using a classical force field. $H_{\text{QM/MM}}$ is the key term which represents the interaction of the MM atom "cores" with the elec-

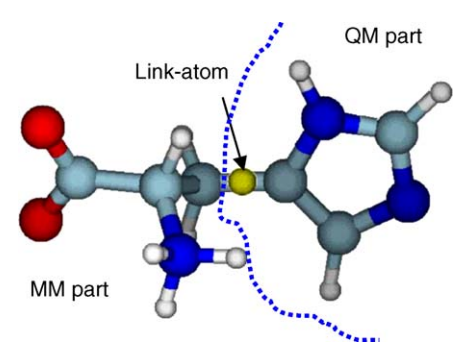

Fig. 5. An example of how to partition a molecule into QM and MM regions. The figure shows a histidine, in which all the atoms in the imidazole ring are taken as QM atoms, while the rest atoms are treated as MM atoms.

tron cloud of the QM atoms, as well as the repulsion between the MM and QM atomic cores, and the Lennard–Jones term cannot be neglected. The form of $H_{QM/MM}$ [13] is:

$$H_{QM/MM} = -\sum_{iM} \frac{q_M}{|r_{iM}|} + \sum_{A} \frac{q_M Z_A}{|R_{AM}|} + \sum_{AM} 4\varepsilon_{AM} \left(\frac{R^{12}_{min,AM}}{R^{12}_{AM}} - 2\frac{R^{6}_{min,AM}}{R^{6}_{AM}} \right) \quad (5)$$

where q_M is the atomic point charge on the MM atom, r_{iM} is the QM electron to MM atom distance, Z_A is the core charge of QM atom A, R_{AM} is the QM atom A to MM atom M distance and ε_{AM} and $R_{min,AM}$ are the Lennard–Jones parameters for QM atoms A interacting with MM atom M. The critical term that allows the QM region to "see" the MM environment is the first term in the right side of Eq. (5) where the summation is over all interactions between MM atoms and QM electrons. The second term in Eq. (5) represents the core-electron interaction between MM and QM atoms and is incorporated into the QM Hamiltonian explicitly. The van der Waals interaction between QM part and MM part is described by the third term in Eq. (5). As the IMOMM method is taken, the introduction of new parameters is avoided and the number of geometry variables is reduced as much as possible.

2.2. Link atoms method

An important aspect of the formation of a hybrid potential is how to handle covalent bonds between atoms that are described with different potentials, and most notably, those bonds exist at the interface of the QM and MM regions. Several methods have been proposed to deal with this problem, ranging from the simple link-atom method [10] to sophisticated hybrid-orbital techniques [24], pseudo-bond approach [25] and some other methods [26–29].

In many situations, it is necessary to split a molecule between QM and MM regions, which means that there are covalent bonds between QM and MM atoms. These cleavage bonds must be treated in some way because the presence of broken bonds and unpaired electrons at the boundary of the QM region dramatically change the electronic structure of the QM subsystem. As long as the QM and MM atoms are in different molecules, no such problem arises.

Here, we introduce the classical link-atom method [10]. The link atoms as shown in Fig. 5 are treated exactly like QM hydrogen atoms in the QM/MM scheme and they are invisible to the MM atoms because no interactions between the link atoms and the MM atoms are calculated. Define the link atoms for each molecule containing both QM and MM atoms. Each bond that crosses the boundary between the two regions must be defined. The link-atom coordinates are determined to place along the bonds between the QM and MM atoms. The exact distance does not matter since the position of the link atoms is optimized in subsequent calculations. The link atoms have no interactions with the MM atoms and appear only in the QM portion of the calculations. They have no entries in any of the nonbond lists. For the IMOMM scheme, the introduction of link atom is modified to study organometallic reactions by subtracting the classical MM interactions with the real QM system.

3. Simulation procedures

The experiment of Conti et al. [9] revealed that both tags could make complex with Ni^{2+} in the different types with different stabilities. In our following work, two, four, six numbers chelate structures are considered, respectively, to investigate the structure and stability of them. Because one of our goals is to investigate the interaction of the His-tags with Ni^{2+} ion, we use a two- partition scheme in the QM/MM calculation. The prepared synthetic peptide–metal–solvent system is partitioned into a QM subsystem and a MM subsystem.

The first part utilizes a smaller QM subsystem consisting of the Ni ion and imidazoles of histidines. For two numbers chelate structure, Ni^{2+} ion and the imidazoles of His_1 and His_3 are included into QM atoms together with four water molecules, with a total of 33 QM atoms. For four numbers chelate structure, Ni^{2+} ion and the imidazoles of His_1 to His_4 together with two molecules are included into QM atoms, with a total of 45 QM atoms. And for six numbers chelate structure, all the imidazole of histidines and Ni^{2+} ion are included without water molecules considered quantumly, for a total of 55 QM atoms. The rest structure consisting of remaining peptide and the solvent are treated as MM part. All the QM part models are shown in Fig. 6.

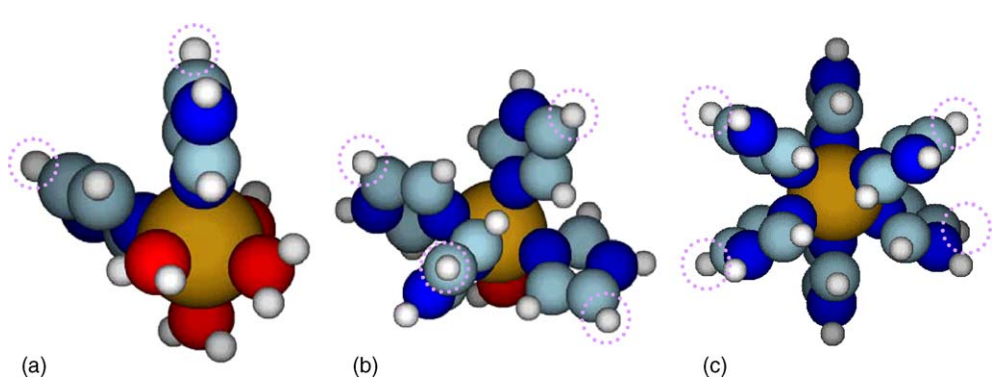

Fig. 6. The QM models of the three chelate structures. The center atom is the Ni^{2+} ion, the hydrogen atoms in the purple dashed circle are the link-atoms to bridge the QM and MM.

The boundary problem between the QM and MM subsystems is treated using the IMOMM approach which can be implemented directly in GAMESS/TINKER calculations.

With these prepared QM/MM systems, full geometry optimizations and energy calculations are performed at the HF (6–31G*)/MM level and B3LYP (6–31G*)/MM level calculations, leading to the optimized structure for the active region. For the QM subsystem, the criteria used for geometry optimizations follow GAMESS default. For the MM subsystem, the convergence criterion used is that the root-mean-square (RMS) energy gradient is less than 0.1 kcal mol^{-1} $Å^{-1}$. In the MM minimization, the Ni ion is fixed only. No cut-off for nonbonded interactions is used in the QM/MM calculations. The force field used in the QM/MM calculation is the MM3 all-atom force field in TINKER for the protein and the TIP3P model for water. For the initial setup, the peptide and Ni^{2+} ion are surrounded by a water box of 20 × 20 × 15 Å containing TIP3P molecules. For the subsequent calculations, a periodic boundary condition (PBC) is employed for the water box. The images of QM section involved in Figs. 3–6 are processed by MOLDEN software [30].

We also perform MD simulations for the synthetic peptide adsorption on Ni(100) surface without ionized region. The Lennard–Jones Parameters of Ni atoms are selected as $\varepsilon = 6030\,K_B$ deg., $\sigma = 2.282$ Å [31]. The MD simulations are done by employing the code CHARMM 28b1 [32]. During the simulation, leapfrog algorithm [33] is used for integrating the Newton's equations of motion for each atom, with a time step of 1 fs. The periodic boundary condition using image conventions is applied in calculating the nonbonded interactions. With a nonbond cut-off 12 Å, the nonbonded pair list is updated every 10 steps, and the nonbonded interaction energies and forces are smoothly shifted to zero at 10 Å. The relative dielectric constant 1.0 for electrostatic calculations is used. As the initial configurations, peptide is placed on the surface of metal with a mean distance about 6 Å. Then the system is equilibrated for 200 ps at 300 K. The temperature is checked every 100 steps, and adjusted by scaling velocities only if the average temperature of the system is outside the range 300 ± 10 K. Thus the average temperature is maintained at 300 K. The size of the water box is kept fixed during the simulation, making it effective under a constant NVT system. To simulate the peeling process of peptide from metal substrate, a dummy atom and the algorithm of constant velocity dynamics are used in the simulation. The dummy atom is linked with the end of the peptide far from the histidine by the constraint function NOE and pulled in the designed direction at a constant velocity. The force constant we used for NOE is $K = 8$ kcal/mol/$Å^2$. With the peeling direction perpendicular to the substrate, pulling rates are selected as 0.1 and 0.01 Å/ps for in aqueous solvent and in vacuum, respectively. During the peeling process, the metal substrate is fixed so that the peeling of the peptide is realized. Similar peeling simulations have been done to study ssDNA adhesion to graphite surface [34] and structural stability of proteins [35].

4. Result and discussion

The binding energy ΔE is defined as:

$$\Delta E = E_{tot}(Ni^{2+} - \text{peptide}) - E_{tot}(Ni^{2+}) - E_{tot}(\text{peptide}), \quad (6)$$

where $E_{tot}(Ni^{2+}$–peptide) is the total energy of the Ni^{2+}–peptide complexes, $E_{tot}(Ni^{2+})$ is the total energy for the Ni^{2+} ion and E_{tot}(peptide) is the total energy of the 6 × his-tagged peptide. The link-atom is introduced into both $E_{tot}(Ni^{2+}$–peptide) and E_{tot}(peptide) calculations, so it rarely affects the ΔE at the end.

The peptide–Ni^{2+} system is fully optimized with the energy of the system approaching the lowest level. Otherwise, more SCF iterations are needed for the bigger QM subsystem. All the geometry parameters and the binding energy are listed in Table 1.

When two histidines of the peptide chelate with the Ni ion, the binding energy of the peptide interaction with Ni ion is −231.626 KJ/mol for the HF(6–31G*)/MM calculation, while the binding energy is about 15 KJ/mol lower for the B3LYP(6–31G*)/MM calculation. The HF calculation scheme is a self-consistent iterative procedure to calculate the Schrödinger equation of a many-electron system in a coulombic potential of fixed nuclei. As a consequence to this, whilst it calculates the exchange energy exactly, it does not calculate the effect of electron correlation at all. While B3LYP schema is a hybrid density functional theory (DFT), which gives approximate solutions to both exchange and correlation energies. So the B3LYP(6–31G*)/MM calculation gets even lower bind-

Table 1
Binding energy and structural data for the optimized chelate structures

	ΔE	D(N–Ni)	D(C1–L)	D(C1–C2)	D(Ni–O)	∠(N–Ni–N)
Two His-tags chelate with Ni^{2+}						
HF(6–31G*)/MM	−231.626	2.056	1.081	1.347	1.962	86.43
B3LYP(6–31G*)/MM	−247.913	2.065	1.083	1.350	1.969	89.62
Four His-tags chelate with Ni^{2+}						
HF(6–31G*)/MM	−314.077	2.083	1.072	1.341	1.973	93.38
B3LYP(6–31G*)/MM	−326.062	2.090	1.075	1.342	1.976	93.40
Six His-tags chelate with Ni^{2+}						
HF(6–31G*)/MM	−382.331	2.092	1.071	1.345	–	91.60
B3LYP(6–31G*)/MM	−399.462	2.095	1.076	1.348	–	92.02
Experiment [37,38]	–	2.112	–	1.355	2.065	93.50

D is the distance, ∠ is the angle (donor atom–Ni^{2+}–donor atom), and L represents the link atom. All distances are in Ångstrom, and energy in KJ/mol.

ing energy, which is surely more precise. The average bond length between the donor atom N and the acceptor atom Ni is 2.065 Å in B3LYP(6–31G*)/MM calculation and 2.056 Å for HF(6–31G*)/MM calculation. The angle of ∠N–Ni–N is a little bit smaller than 90°. The design of two His-tags on the peptide tail chelating with Ni ion of Ni–NTA is widely used in immobilizing a His-tagged bio-molecule on a substrate.

For four and six histidines chelating with Ni ion, the binding energies in corresponding calculations are about 80 and 150 KJ/mol, respectively, which are both lower than the binding energy of two numbers chelation, and the average bond length of N–Ni is increased to about 2.09 Å. The calculated angles ∠N–Ni–N are very close to 90°. It shows that the coordination bonds are close to orthogonal arrangement. The distance between the link-atom and the carbon atom on the QM boundary is initially set as 1 Å and ranges from 1.071 to 1.083 Å in the calculations. This distance has no obvious variation, which shows that the active region does not affect the boundary of QM and MM largely, and vice versa. It shows that the link-atom method is properly involved in these systems. The other geometrical parameters are summarized in this table, too. The bond length of N–Ni is coincident with the high resolution X-ray structure data [36,37]. From the results of the QM/MM calculation, it is known that more energy is needed to break the six numbers chelate structure than the others. The six numbers chelate structure results in the highest binding strength, which is regarded as the most stable structure and enables the His-tagged peptide to be immobilized on ionized nickel surface tightly.

In order to investigate the His-tagged peptide adsorption on neutral Ni surface, we implement classical MD for the adsorption in different environments. For our classical MD, we perform one simulation for peeling the synthetic peptide in aqueous solvent at a constant velocity ($v = 0.01$ Å/ps) and another simulation for the vacuum environment at a constant velocity ($v = 0.01$ Å/ps) ignoring the effect of water molecules. Both the pulling directions are perpendicular to the substrate. We obtain the curves of peeling force versus time for the two simulations shown in Figs. 7 and 8. In the MD simulation, we find that the peptide needs more time for adsorption on the Ni substrate. When the peptide is peeled off from the substrate in aqueous solvent, as shown schematically in Fig. 7, no considerable force is found at the beginning, which means that the several frontal amino acids, GLY and LYS do not adhere to the substrate tightly enough. With the time goes on, the segment with histidines begins to peel off from the substrate, and the force begins to increase. The adhesion force between the peptide and the substrate can be understood more clearly form Fig. 8. The peaks are very obvious in the peeling curve. The maximal force $F_m = 2498$ pN appears when the His_6 is pulled off from the substrate, and another 5 peaks follow in the subsequent peeling whose values are in the range of about 1500–2000 pN, which mean that the binding strength between imidazole of His_6 and the substrate is the highest. These obvious peaks are affirmed to be the sign of pulling off of the imidazoles from the substrate in the peeling movie.

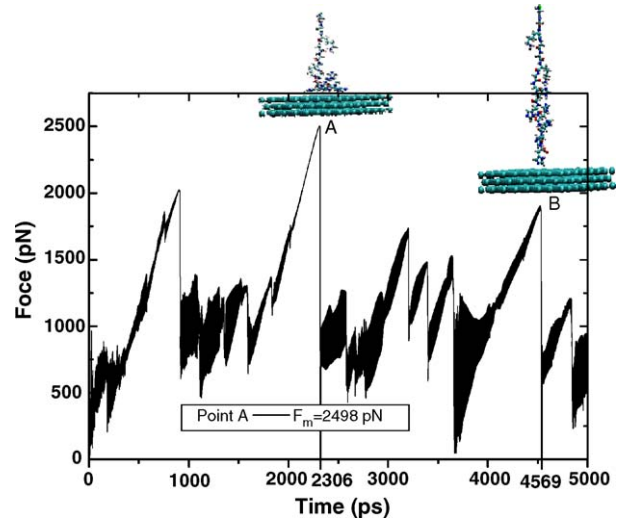

Fig. 8. . Peeling off force of the synthetic peptide adhering to Ni substrate in the vacuum. At point A, the first imidazole is pulled off from the substrate and $F_m = 2498$ pN; At point B, the last imidazole is pulled off from the substrate.

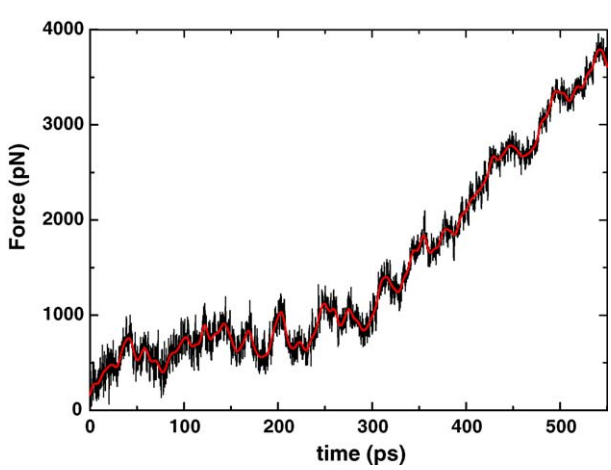

Fig. 7. Peeling off force of the synthetic peptide adhering to Ni substrate in aqueous solvent. To eliminate thermal noise, the pulling force is filtered with a 100 point FFT smoothing (red line).

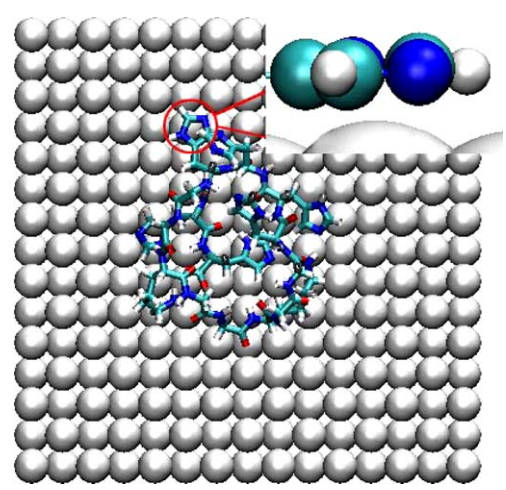

Fig. 9. The His-tagged peptide adhering to the Ni(1 0 0) surface with about half of the imidazoles parallel with the substrate after 10 ns equilibrium. The imidazole in red circle is viewed from side.

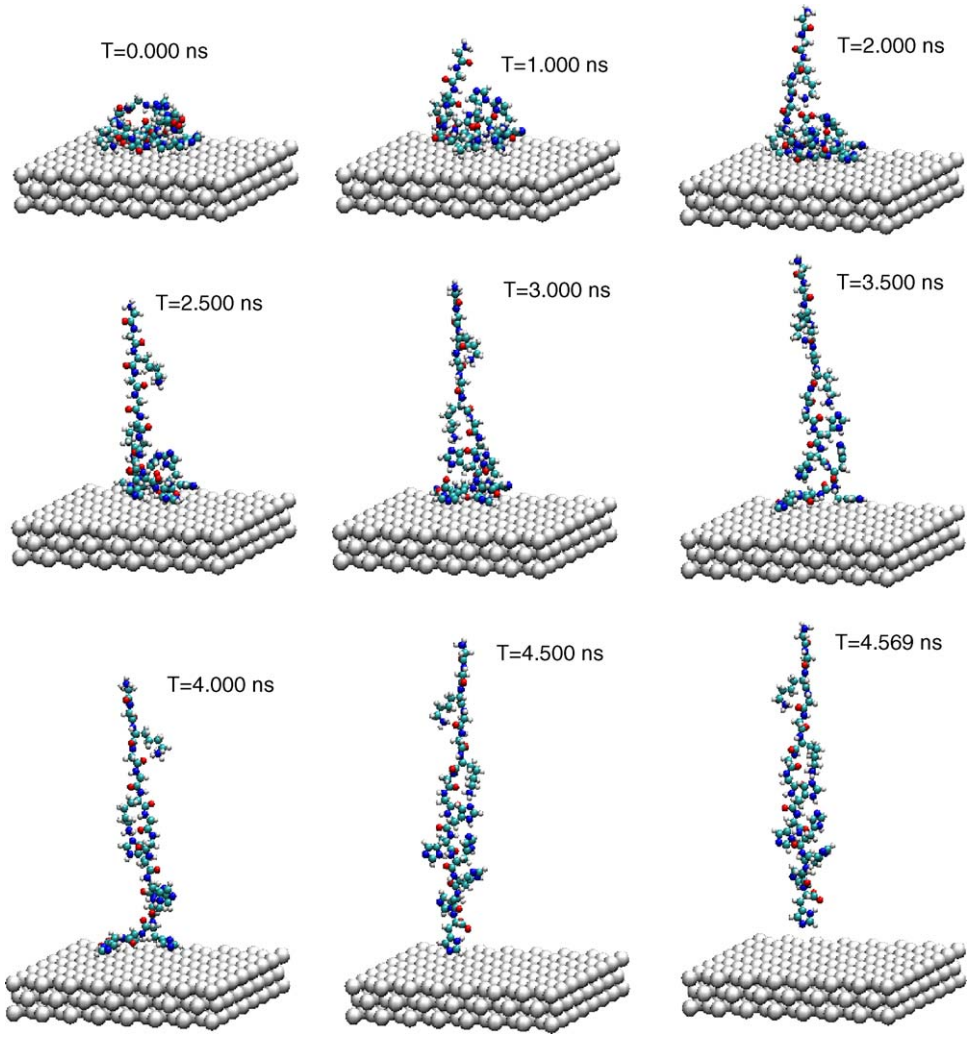

Fig. 10. Peeling the synthetic peptide from the Ni substrate in vacuum at a constant velocity 0.01 Å/ps.

When the synthetic peptide adheres to the substrate, the ringed structure, imidazoles, always trend to become parallel with the substrate by the energy approaching to equilibrium, but not all of the imidazoles can be parallel with the substrate at the end of 10 ns equilibrium, which is shown in Fig. 9. The average distance between the imidazole rings and the Ni substrate is about 3.85 Å in the aqueous environment and 3.25 Å in the vacuum. The structures of imidazole rings in parallel with the substrate make the interaction area bigger, which leads to stronger adhesion. Fig. 10 shows the process of peeling the synthetic peptide off from the substrate in the vacuum. This image of MD result was processed by VMD software [38]. These pictures show that the imidazoles play a very important role in the adhesion and result in the peaks in the curve of Fig. 8. His_6 is already apart from the substrate at the time $T = 2.5$ ns, which is pulled off at the time $T = 2.306$ ns. During the peeling, the conformation of the synthetic peptide changes as the amino acids are pulled off from the substrate. During the time $T = 3.0$ to $T = 3.5$ ns, the His_3 that does not attach to the substrate before peeling, adheres to the substrate and then is pulled off. The final base His_1 is pulled off from the substrate at the time $T = 4.569$ ns. The orientation of imidazole ring of His_1 changes from being parallel with the substrate to being perpendicular to the substrate and left the substrate at last.

5. Conclusions

The QM/MM simulation results show the $6 \times$ His-tagged peptide can form the most stable structure with high binding energy which is also affirmed experimentally [8]. And the optimized structure data are obtained satisfactorily. The results obtained for the peptide–Ni chelate complexes also show that the present QM/MM approach is reasonable and effective. Such delicate properties as conformational changes and binding energy are modeled in our QM/MM calculations.

It is shown that the QM/MM method can be used to probe aspects of metal chelate complexes from both fundamental and practical aspects. And by classical MD simulation, it can be realized that half of imidazoles of the His-tags are almost parallel with the substrate so as to enhance the binding strength.

Understanding how polymer molecules behave near metal surfaces would greatly enhance our ability to control the essen-

tial interfacial properties in a wide variety of problems, including adhesion, wetting and nanowetting, biomolecular recognition, and self-assembly. Such understanding is, however, difficult to be obtained by experiment directly. Specifically, atomic-scale energetics dominates at the interface, where chemisorption and physisorption of different small parts of the polymer molecules may occur. The QM/MM method is a powerful and effective tool to investigate the polymer interaction with metals.

Acknowledgements

This research was supported by the National Natural Science Foundation of China (NSFC) (grant No. 10225209 and No. 90305020), key project from the Chinese Academy of Sciences (grant No. KJCX2-SW-L2).

References

[1] H. Noji, R. Yasuda, M. Yoshida, K. Kinosita Jr., Nature 386 (1997) 299–302.
[2] C. Montemagno, G. Bachand, Nanotechnology 10 (1999) 225–231.
[3] E. Hochuli, H. DoBeli, A. Schacher, J. Chromatogr. 411 (1987) 177–184.
[4] J. Crowe, H. Döbeli, R. Gentz, E. Hochuli, D. Stüber, Methods Mol. Biol., Humanna Press, Totowa, NJ 31 (1994) 371–387.
[5] R.G. Nuzzo, D.L. Allara, J. Am. Chem. Soc. 105 (1983) 4481–4483.
[6] L.M. Demers, D.S. Ginger, S.J. Park, Z. Li, S.W. Chung, C.A. Mirkin, Science 296 (2002) 1836–1838.
[7] G. Agarwal, R.R. Naik, M.O. Stone, J. Am. Chem. Soc. 125 (2003) 7408–7412.
[8] L. Schmitt, M. Ludwig, H.E. Gaub, R. Tampé, Biophys. J. 78 (2000) 3275–3285.
[9] M. Conti, G. Falini, B. Samori, Angew. Chem. Int. Ed. 39 (2000) 215–218.
[10] M.J. Field, P.A. Bash, M. Karplus, J. Comput. Chem. 11 (1990) 700–733.
[11] M.W. Schmidt, K.K. Baldridge, J.A. Boatz, S.T. Elbert, M.S. Gordon, J.H. Jensen, S. Koseki, N. Matsunaga, K.A. Nguyen, S. Su, T.L. Windus, M. Dupuis, J.A. Montgomery Jr., J. Comput. Chem. 14 (1993) 1347–1363.
[12] J.W. Ponder, TINKER, Software Tools for Molecular Design, URL http://dasher. wustl. edu/tinker.
[13] F. Marseras, K. Morokuma, J. Comput. Chem. 16 (1995) 1170–1179.
[14] F. Maseras, Chem. Commun. (2000) 1821–1827.
[15] I.S.Y. Wang, M. Karplus, J. Am. Chem. Soc. 95 (1973) 8160–8164.
[16] J.H. McCreery, R.E. Christoffersen, G.G. Hall, J. Am. Chem. Soc. 98 (1976) 7191–7197.
[17] V. Luzhkov, A. Warshel, J. Comput. Chem. 13 (1992) 199–213.
[18] J.L. Gao, P. Amara, C. Alhambra, M.J. Field, J. Phys. Chem. A 102 (1998) 4714–4721.
[19] A.D. Becke, J. Chem. Phys. 98 (1993) 5648–5652.
[20] P.J. Stephens, F.J. Devlin, C.F. Chabalowski, M.J. Frisch, J. Phys. Chem. 98 (1994) 11623–11627.
[21] R.H. Hertwig, W. Koch, Chem. Phys. Lett. 268 (1997) 345–351.
[22] P.D. Lyne, M. Hodoscek, M. Karplus, J. Phys. Chem. A 103 (1999) 3462–3471.
[23] K.M. Merz Jr., ACS Symp. Series 712 (1998) 2–15.
[24] N. Ferré, X. Assfeld, J.L. Rivail, J. Comput. Chem. 23 (2002) 610–624.
[25] Y.K. Zhang, T.S. Lee, W.T. Yang, J. Chem. Phys. 110 (1999) 46–54.
[26] X. Assfeld, J.L. Rivail, Chem. Phys. Lett. 263 (1996) 100–106.
[27] F. Maseras, K. Morokuma, J. Comput. Chem. 16 (1995) 1170–1179.
[28] J.C. Corchado, D.G. Truhlar, J. Phys. Chem. A 102 (1998) 1895–1898.
[29] G.A. DiLabio, M.M. Hurley, P.A. Christiansen, J. Chem. Phys. 116 (2002) 9578–9584.
[30] G. Schaftenaar, J.H. Noordik, J. Comput. -Aided Mol. Des. 14 (2000) 123–134.
[31] D. Stauffer, Annual Reviews Comput. Phys. IX, Cologne University, Germany, 2001, pp. 10–11.
[32] B.R. Brooks, R.E. Bruccoleri, B.D. Olafson, D.J. States, S. Swaminathan, M. Karplus, J. Comput. Chem. 4 (1983) 187–217.
[33] R.W. Honeycutt, Methods Comput. Phys. 9 (1970) 136–211.
[34] X.H. Shi, Y. Kong, Y.P. Zhao, H.J. Gao, Acta Mech. Sinica 21 (2005) 249–256.
[35] J. Yin, Y.P. Zhao, R.Z. Zhu, Mater. Sci. Eng. A 409 (2005) 160–166.
[36] P.A. Petrenko, M. Gdaniec, Yu A. Simonov, V.G. Stavila, A.P. Gulea, Russian J. Coordination Chem. 30 (2004) 813–817.
[37] C. Arici, F. Ercan, O. Atakol, Ö. Başgut, Anal. Sci. 18 (2002) 375–376.
[38] W. Humphrey, A. Dalke, K. Schulten, J. Mol. Graph. 14 (1996) 33–38.